# Performance Comparison of Auxiliary Vector and RAKE-MF Receiver for Transport of H.264/AVC Video Over DS-CDMA Wireless Channels

Anand V.S. Mantravadi, Pavan Venugopal, Lisimachos P. Kondi
University at Buffalo, The State University of New York, NY 14260.
Email:{sm236, pv9, lkondi}@ eng.buffalo.edu

***Abstract*— In this paper, we propose a robust transmission technique for packet-based H.264/AVC video transmission over DS-CDMA wireless channels using Auxiliary Vector (AV) and RAKE-MF receivers and confirm the superiority of the AV receiver. AV Filtering is an iterative algorithm that has fast convergence for short data records. In the proposed system, the H.264 video data packets are packetized and transported as per the RTP/UDP/IP protocol stack over a CDMA wireless physical layer link. Techniques like Packet Interleaving at NAL layer and Optimal Buffering at the link layer are been proposed and implemented to resolve the inherent tradeoff and improve the efficiency of the system without compromising on the real-time transmission bounds. We present results which confirm the superiority of the Auxiliary Vector over the RAKE-MF receiver for a wide range of user SNR and channel coding rates in terms of output video quality for two different video sequences. An optimal system for transmission of packet based H.264 video over CDMA wireless links has been designed and implemented under this context.**

## I. Introduction

H.264/AVC [1] is a new video coding standard that has tremendous potential to be utilized in a wide range of areas like video transmission, conferencing and storage because it not only offers excellent compression efficiency but also easy integration of the encoded video into current and future transport media. It introduces the idea of distinguishing between the two conceptual layers, the Video Coding layer (VCL) and the Network Adaptation Layer (NAL). The former is concerned with the efficient encoding of the video and the latter defines an interface between the encoded video and the transport media. The VCL employs techniques like integer transforms, multiple block size motion estimation, multi-frame motion prediction, quarter pixel motion accuracy, different intra encoding modes, Context Adaptive Binary Arithmetic Coding (CABAC), Deblocking filter etc. to achieve high compression efficiency up to half the bit rate for the same video quality compared to previous standards [2]. The interface between VCL and NAL is obtained by the slice layer. Slice is a group of macroblocks which forms the fundamental data structure of the VCL and can be decoded independently. A NAL [3] represents a slice encoded data along with additional headers. The NAL is responsible for encapsulation of VCL packets into so-called NAL units for transparent delivery over heterogeneous networks, framing, timing issues, and synchronization. Currently the most well defined NAL is for the IP/UDP/RTP [4]-[5] based networks and the same has been considered in this paper.

Design of robust systems for transport of H.264/AVC video DS-CDMA wireless links is of great interest. In this paper we have designed a robust packet based transmission system and under this setup we have given a performance comparison of Auxiliary Vector (AV) Filtering and the conventional RAKE-MF receiver. AV Filtering is an iterative algorithm that starts at the RAKE-MF filter and generates an infinite sequence of filters before converging to the ideal MVDR filter. However this algorithm has been shown to have fast convergence when compared to LMS, RLS and other online adaptive schemes for short data records and thus is extremely efficient when compared to the conventional RAKE-MF receiver. Section II gives a complete detail of the proposed transmission system. Section III describes the Auxiliary Vector algorithm and the underlying mathematics. Simulation parameters and results are discussed in detail in Section IV.

## II. Video Transmission System

In the proposed system, the encoded video data packets or the NAL units generated by the reference H.264 encoder software are packetized as per the RTP/UDP/IP protocol stack. Figure 1 gives a overview of the system proposed in this paper.

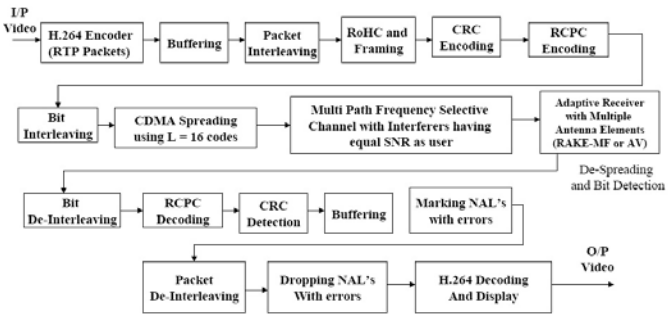


**Fig. 1:** Transmission System Block Diagram

After Robust Header Compression (ROHC) [6] we have to create constant size frames for transmission over the underlying wireless link. In our simulations we chose a size of 100 bytes which is a regular size for such wireless systems [7]. Each of these frames is attached with a Cyclic Redundancy Check (CRC) header [8] for error detection and are then channel encoded using Rate Compatible Punctured Convolutional Codes (RCPC) [9]. RCPC codes have been considered to investigate the performance of the system for different channel protection. The channel encoded frames is then spreaded using Walsh Hadamard code of length "L = 16" and is transmitted over a multipath Rayleigh fading channel with Additive White Gaussian Noise (AWGN) and interference. The received data are despread/demodulated using the Auxiliary Vector (AV) receiver or conventional RAKE matched filter (RAKE-MF) receiver with multiple antenna elements and, subsequently, channel and source decoded.

### A. Optimal Buffering at Link Layer

Video packets or the NAL units are of varying lengths by nature depending upon the encoded video content and hence the need to create constant size frames calls for padding unnecessary bits to the video data. Clearly, the most error resilient way is to pad each packet so that the loss of a single frame will effect only one NAL unit. However it was found in our simulations that such framing will lead to excessive padding bits upto the order of 40% to 50% of the useful data. The solution to this is to consider the NAL units in a continuous sequence by buffering several NAL units and perform the framing over the data in the buffer. Intuitively, we can see that, for a large buffer size the padding bits will be reduced, but the decoder has to wait for the entire data belonging to at least one frame before it can decode the NAL units and display the frame, thus disturbing real-time streaming. We have investigated the behavior of the ratio of the padding bits to useful data as we change the buffer size expressed in terms of number of consecutive frames whose NAL's are in the buffer. For example if the buffer size is four, it indicates the buffer can accommodate NAL units belonging to four frames. Figure 2 gives this curve for both Foreman (solid line) and Akiyo (dashed line) QCIF sequences encoded in IP mode for different link layer frame sizes.

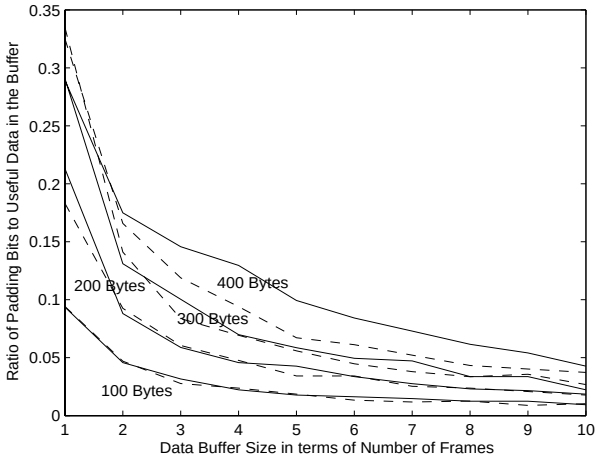


**Fig. 2:** Ratio of Padding Bits to Buffer Size in Number of Frames for IP Encoding for Foreman and Akiyo Sequences for Different Link Layer Frame Sizes

Analyzing this graph for a frame size of 100 bytes, we see that there is not much improvement in reducing the padding bits after a buffer size of five frames. The same is observed for all the video sequences simulated and also for different link layer frame sizes. Thus, we chose to have a buffer size of five frames which turned to be optimal in our setup.

### B. Packet Interleaving

As discussed in II-A, if we are using a buffer to have a continuous flow of packets and reduce the padding bit overhead, then the loss of a single link layer frame can result in the loss of two successive IP level packets or NAL units. Thus, there is a possibility of a burst packet loss at the IP level, which is undesirable. To avoid this, we introduce a packet level interleaver, which scrambles the IP packets in the buffer in an predefined manner before the link layer framing is done. This separates successive NAL units and hence reduces the possibility of a burst loss of packets.

Depth of the interleaver is defined as the number of packets that come between two successively numbered packets. Clearly the greater the depth of the interleaver, the higher is the protection but it introduces more delay. In our system setup addition of packet interleaving forces the decoded to wait for the data in the entire buffer before it can decode. Since the buffer size was chose optimally, this additional delay is not an overhead compared to the performance gain seen by this interleaving scheme. Hence the depth of the interleaver in our simulations were chosen to be the maximum allowed as per the buffer size.

### C. Received Signal

We model the baseband received signal at each antenna element $m$, $m = 1, \ldots, M$, as the aggregate of the received multipath spread-spectrum (SS) signal of interest with signature code $\mathbf{S}_o$ of length $L$ (if $T$ is the symbol period and $T_c$ is the chip period then $L = T/T_c$), $K-1$ received DS-SS interferers with unknown signatures $\mathbf{S}_k$, $k = 1, ..., K-1$, and white Gaussian noise. For notational simplicity and without loss of generality, we adopt a chip-synchronous signal formulation. We assume that the multipath spread is of the order of a few chip intervals, $P$, and since the signal is bandlimited to $B = 1/2T_c$. The lowpass channel can be represented as a tapped delay line with $P+1$ taps spaced at chip intervals $T_c$. After conventional chip-matched filtering and sampling at the chip rate over a multipath extended symbol interval of $L+P$ chips, the $L+P$ data samples from the $m$th antenna element, $m = 1, \ldots, M$, are organized in the form of a vector $\mathbf{r}_m$ given by

$$\mathbf{r}_m = \sum_{k=0}^{K-1} \sum_{p=0}^{P} c_{k,p}\sqrt{E_k}(b_k \mathbf{s}_{k,p} + b_k^- \mathbf{s}_{k,p}^- + b_k^+ \mathbf{s}_{k,p}^+)\mathbf{a}_{k,p}[\mathrm{m}] + \mathbf{n} \ , \tag{1}$$

where, with respect to the $k$th CDMA signal, $E_k$ is the transmitted energy per chip, $b_k$, $b_k^-$, and $b_k^+$ are the present, the previous, and the following transmitted bit, respectively, and $\{c_{k,p}\}$ are the coefficients of the frequency-selective slowly fading (quasi-static) channel modeled as independent zero-mean complex Gaussian random variables that are assumed to remain constant over a few symbol intervals. $\mathbf{s}_{k,p}$ represents the 0-padded by $P$, $p$-cyclic-shifted version of the signature of the $k$th SS signal $\mathbf{s}_k$, $\mathbf{s}_{k,p}^-$ is the 0-filled $(L-p)$-left-shifted version of $\mathbf{s}_{k,0}$, and $\mathbf{s}_{k,p}^+$ is the 0-filled $(L-p)$-right-shifted version of $\mathbf{s}_{k,0}$. Finally, $\mathbf{n}$ represents additive complex Gaussian noise with mean $\mathbf{0}$ and autocorrelation matrix $\sigma^2\mathbf{I}_M$, and $\mathbf{a}_{k,p}[\mathrm{m}]$ is the $m$th coordinate of the $k$th CDMA signal, $p$th path, array response vector:

$$\mathbf{a}_{k,p}[\mathrm{m}] = e^{j2\pi(m-1)\frac{\sin\theta_{k,p}d}{\lambda}} \ , \ m = 1, \ldots, M, \tag{2}$$

where $\theta_{k,p}$ identifies the angle of arrival of the $p$th path of the $k$th CDMA signal, $\lambda$ is the carrier wavelength, and $d$ is the element spacing (usually $d = \lambda/2$).

To avoid in the sequel cumbersome 2-D data notation and filtering operations, we decide at this point to "vectorize" the $(L+P) \times M$ space-time data matrix $[\mathbf{r}_1 \ \mathbf{r}_2 \ \cdots \ \mathbf{r}_M]$ by sequencing all matrix columns in the form of a single $(L+P)M$-long column vector:

$$\mathbf{r}_{(\mathrm{L+P})\mathrm{M}\times 1} = Vec\{[\mathbf{r}_1, \ \mathbf{r}_2, \ \cdots, \ \mathbf{r}_M]_{(\mathrm{L+P})\times \mathrm{M}}\} \ . \tag{3}$$

From now on, $\mathbf{r}$ denotes the joint space-time data in the $\mathcal{C}^{(L+P)M}$ complex vector domain. For conceptual and notational simplicity we may rewrite the vectorized space-time data equation as follows:

$$\mathbf{r} = \sqrt{E_0} b_0 \mathbf{w}_{\text{R-MF}} + \mathbf{i} + \mathbf{n} \tag{4}$$

where $\mathbf{w}_{\text{R-MF}} = E_{b_0}\{\mathbf{r}\, b_0\} = Vec\{[\sum_{p=0}^{P} c_{0,p}\mathbf{s}_{0,p}, \mathbf{a}_{0,p}[1], \cdots, \cdots, \sum_{p=0}^{P} c_{0,p}\mathbf{s}_{0,p}\mathbf{a}_{0,p}[\mathrm{M}]\,]\}$ is the effective space-time signature of the CDMA signal of interest (signal *0*) and $\mathbf{i}$ identifies comprehensively both the inter-symbol and the CDMA interference present in $\mathbf{r}$ ($E_{b_0}\{\cdot\}$ denotes statistical expectation with respect to $b_0$). We use the subscript R-MF in our effective S-T signature notation to make a direct association with the RAKE matched-filter time-domain receiver that is known to correlate the signature $\mathbf{s_0}$ with $P+1$ size-$L$ shifted windows of the received signal (that

correspond to the $P+1$ paths of the channel), appropriately weighted by the conjugated channel coefficients $c_{0,p}, p = 0, \ldots, P$. In our notation, the generalized S-T RAKE-MF operation corresponds to linear filtering of the form $\mathbf{w}_{\text{R-MF}}^{\text{H}}\mathbf{r}$, where $H$ denotes the Hermitian operation.

## III. Auxiliary Vector Filtering Algorithm

The AV algorithm generates an infinite sequence of filters $\{\mathbf{w}_k\}_{k=0}^{\infty}$. The sequence is initialized at the S-T RAKE filter

$$\mathbf{w}_0 = \frac{\mathbf{w}_{\text{R-MF}}}{\|\mathbf{w}_{\text{R-MF}}\|^2}, \tag{5}$$

which is here scaled to satisfy $\mathbf{w}_0^H \mathbf{w}_{\text{R-MF}} = 1$. At each step $k+1$ of the algorithm, $k = 0, 1, 2, \ldots$, an "auxiliary" vector component $\mathbf{g}_{k+1}$ that is orthogonal to $\mathbf{w}_{\text{R-MF}}$ is incorporated in $\mathbf{w}_k$ and weighted by a scalar $\mu_{k+1}$ to form the next filter in the sequence,

$$\mathbf{w}_{k+1} = \mathbf{w}_k - \mu_{k+1}\mathbf{g}_{k+1}. \tag{6}$$

The auxiliary vector $\mathbf{g}_{k+1}$ is chosen to maximize, under fixed norm, the magnitude of the cross-correlation between its output, $\mathbf{g}_{k+1}^H\mathbf{r}$, and the previous filter output, $\mathbf{w}_k^H\mathbf{r}$, and is given by

$$\mathbf{g}_{k+1} = \mathbf{R}\mathbf{w}_k - \frac{\mathbf{w}_{\text{R-MF}}^H \mathbf{R}\mathbf{w}_k}{\|\mathbf{w}_{\text{R-MF}}\|^2}\mathbf{w}_{\text{R-MF}} \tag{7}$$

where $\mathbf{R}$ is the input autocorrelation matrix, $\mathbf{R} = E\{\mathbf{r}\mathbf{r}^H\}$. The scalar $\mu_{k+1}$ is selected such that it minimizes the output variance of the filter $\mathbf{w}_{k+1}$ or equivalently minimizes the mean-square (MS) error between $\mathbf{w}_k^H\mathbf{r}$ and $\mu_{k+1}^*\mathbf{g}_{k+1}^H\mathbf{r}$. The MS-optimum $\mu_{k+1}$ is

$$\mu_{k+1} = \frac{\mathbf{g}_{k+1}^H \mathbf{R}\mathbf{w}_k}{\mathbf{g}_{k+1}^H \mathbf{R}\mathbf{g}_{k+1}}. \tag{8}$$

The AV filter recursion is completely defined by (5)-(8). More detailed discussion is given in [10] and [11]. Theoretical analysis of the AV algorithm was pursued in [12] and summarized in this theorm.

*Theorem 1:* Let $\mathbf{R}$ be a Hermitian positive definite matrix. Consider the iterative algorithm of eqs. (5)-(8).
*(i)* Successive auxiliary vectors generated through (6)-(8) are orthogonal: $\mathbf{g}_k^H \mathbf{g}_{k+1} = 0$, $k = 1, 2, 3, \ldots$ (however, in general $\mathbf{g}_k^H \mathbf{g}_j \neq 0$ for $|k-j| \neq 1$).
*(ii)* The generated sequence of auxiliary-vector weights $\{\mu_k\}$, $k = 1, 2, \ldots$, is real-valued, positive, and bounded: $0 < \frac{1}{\lambda_{\max}} \leq \mu_k \leq \frac{1}{\lambda_{\min}}$, $k = 1, 2, \ldots$, where $\lambda_{\max}$ and $\lambda_{\min}$ are the maximum and minimum, correspondingly, eigenvalues of $\mathbf{R}$.
*(iii)* The sequence of auxiliary vectors $\{\mathbf{g}_k\}$, $k = 1, 2, \ldots$, converges to the $\mathbf{0}$ vector: $\lim_{n\to\infty} \mathbf{g}_n = \mathbf{0}$.
*(iv)* The sequence of auxiliary-vector filters $\{\mathbf{w}_k\}$, $k = 1, 2, \ldots$, converges to the minimum-variance-distortionless-response (MVDR) filter: $\lim_{k\to\infty} \mathbf{w}_k = \frac{\mathbf{R}^{-1}\mathbf{w}_{\text{R-MF}}}{\mathbf{w}_{\text{R-MF}}^H \mathbf{R}^{-1}\mathbf{w}_{\text{R-MF}}}$. □

If $\mathbf{R}$ is unknown and sample-average estimated from a packet data record of $D$ points, $\hat{\mathbf{R}}(D) = \frac{1}{D}\sum_{d=1}^{D} \mathbf{r}_d\mathbf{r}_d^H$, then we have

$$\hat{\mathbf{w}}_k(D) \underset{k\to\infty}{\longrightarrow} \hat{\mathbf{w}}_\infty(D) = \frac{\left[\hat{\mathbf{R}}(D)\right]^{-1}\mathbf{w}_{\text{R-MF}}}{\mathbf{w}_{\text{R-MF}}^H\left[\hat{\mathbf{R}}(D)\right]^{-1}\mathbf{w}_{\text{R-MF}}} \tag{9}$$

where $\hat{\mathbf{w}}_\infty(D)$ is the widely used MVDR filter estimator known as the sample-matrix-inversion (SMI) filter [13]. The output sequence begins from $\hat{\mathbf{w}}_0(D) = \frac{\mathbf{w}_{\text{R-MF}}}{\|\mathbf{w}_{\text{R-MF}}\|^2}$, which is a *0*-variance, fixed-valued, estimator that may be severely biased ($\hat{\mathbf{w}}_0(D) = \frac{\mathbf{w}_{\text{R-MF}}}{\|\mathbf{w}_{\text{R-MF}}\|^2} \neq \mathbf{w}_{\text{MVDR}}$) unless $\mathbf{R} = \sigma^2\mathbf{I}$ for some $\sigma > 0$. In the latter trivial case, $\hat{\mathbf{w}}_0(D)$ is already the perfect MVDR filter. Otherwise, the next filter estimator in the sequence, $\hat{\mathbf{w}}_1(D)$, has a significantly reduced bias due to the optimization procedure employed at the expense of non-zero estimator (co-)variance. As we move up in the sequence of filter estimators $\hat{\mathbf{w}}_k(D)$, $k = 0, 1, 2, \ldots$, the bias decreases rapidly to zero while the variance rises slowly to the SMI ($\hat{\mathbf{w}}_\infty(D)$) levels.

An adaptive data-dependent procedure for the selection of the most appropriate member of the AV filter estimator sequence $\{\hat{\mathbf{w}}_k(D)\}$ for a given data record of size $D$ is presented in [14]. The procedure selects the estimator $\hat{\mathbf{w}}_k$ from the generated sequence of AV filter estimators that exhibits maximum J-divergence between the filter output conditional distributions given that $+1$ or $-1$ is transmitted. Under a Gaussian approximation on the conditional filter output distribution, it was shown in [14] that the J-divergence of the filter estimator with $k$ auxiliary vectors is

$$J(k) = \frac{4\,E^2\left\{b_0 \text{Re}\left[\hat{\mathbf{w}}_k^H(D)\mathbf{r}\right]\right\}}{Var\left\{b_0 \text{Re}\left[\hat{\mathbf{w}}_k^H(D)\mathbf{r}\right]\right\}}. \tag{10}$$

To estimate the J-divergence $J(k)$ from the data packet of size $D$, the transmitted information bits $b_0$ are required to be known. A blind *approximate* version of $J(k)$ can be obtained by substituting the information bit $b_0$ in (10) by the detected bit $\hat{b}_0 = \text{sgn}\left(\text{Re}\left\{\hat{\mathbf{w}}_k^H(D)\mathbf{r}\right\}\right)$ (output of the sign detector that follows the linear filter). In particular, using $\hat{b}_0$ in place of $b_0$ in (10) gives the following J-divergence expression:

$$J_B(k) = \frac{4\,E^2\left\{\hat{b}_0 \text{Re}\left[\hat{\mathbf{w}}_k^H(D)\mathbf{r}\right]\right\}}{Var\left\{\hat{b}_0 \text{Re}\left[\hat{\mathbf{w}}_k^H(D)\mathbf{r}\right]\right\}} = \frac{4\,E^2\left\{\left|\text{Re}\left[\hat{\mathbf{w}}_k^H(D)\mathbf{r}\right]\right|\right\}}{Var\left\{\left|\text{Re}\left[\hat{\mathbf{w}}_k^H(D)\mathbf{r}\right]\right|\right\}} \tag{11}$$

where the subscript "B" identifies the blind version of the J-divergence function. To estimate $J_B(k)$ from the data packet of size $D$, we substitute the statistical expectations in (11) by sample averages.

## IV. Simulation Parameters and Results

The "Foreman" and "Akiyo" QCIF sequences were encoded at a bit rate of 60kbps with an intra frame refresh after 30 frames period and 15 fps of frame rate in I-P format using the JM 9.6 version of the H.264 reference software. Each frame was divided into 9 NALs for robust transmission. This led to a choice of the interleaver depth to be 15. The allowed channel coding rates were 1/3, 1/2, 2/3, 4/5 and 8/9. Walsh-Hadamard codes of length "L = 16" were used as spreading codes. We considered a multipath Rayleigh fading channel with three resolvable multipaths and nine interferers with the same SNR as the user of interest. AV and RAKE-MF filters were used at the receiver with four antenna elements.

Figure 3 and 4 give the packet loss probability for RAKE-MF and AV receiver respectively. We can clearly see the spectacular performance of the AV receiver especially in the range of SNR's seen in practice. The packet loss probablity is almost zero for SNR's greater than 12dB and this is an excellent performance improvement over RAKE-MF. Figure 5 and 6 gives the comparison of the average PSNR of the received video for RAKE-MF and AV receivers for both "Foreman" and "Akiyo" sequences for channel rates of 1/3, 2/3 and 8/9. We see that for all channel rate and SNR's, the performance of AV receiver is much better than RAKE-MF receiver especially for large SNR's where the packet loss probability of the AV receiver almost goes to zero. The same performance was observed with other channel rates as well. The results presented below completely prove that the Auxiliary Vector filtering receiver outperforms the RAKE-MF receiver for all channel encoding rates, SNR and video encoding modes. Finally, the proposed system is optimal for the transmission of packet based H.264 video over DS-CDMA wireless channels. Since H.264 is expected to become the future standard in video coding, the proposed system is of great importance in the field of wireless video transmission.

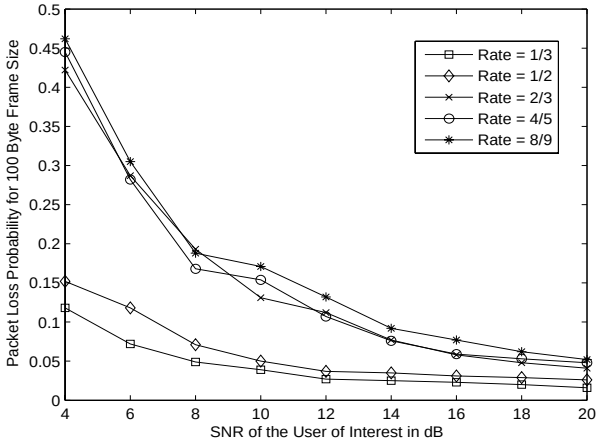


**Fig. 3:** Packet Loss Rate for RAKE-MF Receiver for frame size of 100 bytes

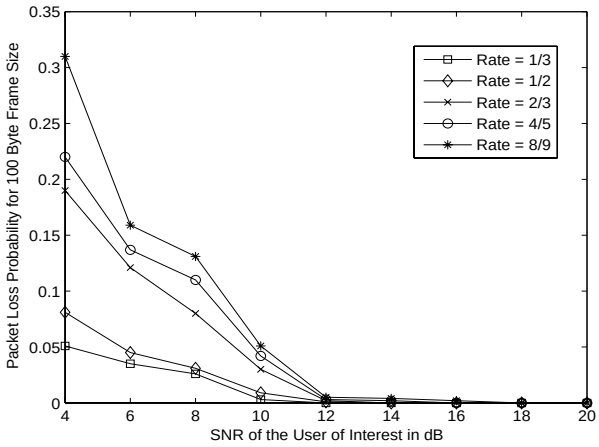


**Fig. 4:** Packet Loss Rate for AV Receiver for frame size of 100 bytes

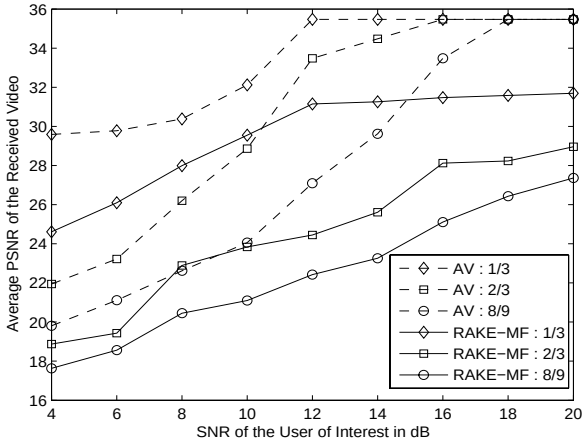


**Fig. 5:** Comparison of Auxiliary Vector Filtering and RAKE-MF Receiver for Foreman Sequence in **IP** Encoding Mode for Different Channel Rates

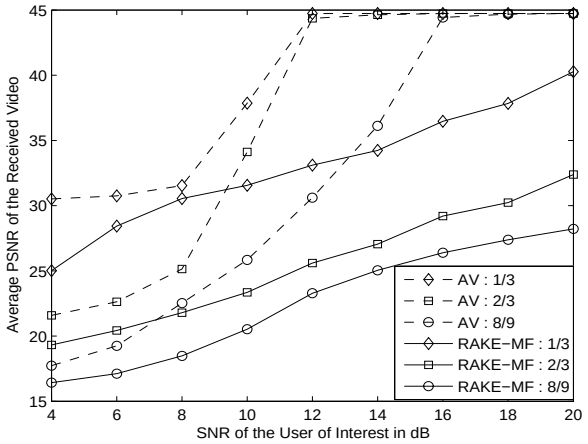


**Fig. 6:** Comparison of Auxiliary Vector Filtering and RAKE-MF Receiver for Akiyo Sequence in **IP** Encoding Mode for Different Channel Rates

## REFERENCES


[1] T. Wiegand, "Final committee draft: Editors proposed revisions," tech. rep., Joint Video Team (JVT) of ISO/IEC MPEG and ITU-T VCEG, Feb 2003.

[2] T. Wiegand, G. J. Sullivan, G. Bjontegaard, and A. Luthra, "Overview of the H.264/AVC video coding standard," in *IEEE Transactions on Circuits and Systems for Video Technology*, **13**, pp. 560 – 576, July 2003.

[3] T. Stockhammer, M. M. Hannuksela, and S. Wenger, "H.26L/JVT Coding Network Abstraction Layer and IP-Based Transport," in *ICIP - International Conference on Image Processing*, 2002.

[4] S. Wenger, "H.264/AVC over IP," in *IEEE Transactions on Circuits and Systems for Video Technology*, **13**, pp. 645 – 656, July 2003.

[5] H. Schulzrinne, S. Casner, R. Frederick, and V. Jacobson, "RTP: A Transport Protocol for Real-Time Applications," *RFC 1889* , 1996.

[6] H. Hannu, L. E. Jonsson, R. Hakenberg, T. Koren, K. Le, Z. Liu, A. Martensson, A. Miyazaki, K. Svanbro, T. Wiebke, T. Yoshimura, and H. Zheng, "Robust header compression (ROHC): Framework and four profiles: RTP, UDP, ESP and Uncompressed," *RFC 3095* , July 2001.

[7] T. Stockhammer, M. H. Hannuksela, and T. Wiegand, "H.264/AVC in Wireless Environments," in *IEEE Transactions on Circuits and Systems for Video Technology*, **13**, pp. 657 – 673, July 2003.

[8] W. H. Press, B. P. Flannery, S. A. Teukolsky, and W. T. Vetterling, *Cyclic Redundancy and Other Checksums*, ch. 20.3, pp. 888–895. Cambridge, England: Cambridge University Press, 1992.

[9] J. Hagenauer, "Rate-Compatible Punctured Convolutional Codes (RCPC codes) and their Applications," in *IEEE Trans. Comm.*, **36**, pp. 389 – 399, April 1988.

[10] A. Kansal, S. N. Batalama, and D. A. Pados, "Adaptive maximum SINR RAKE filtering for DS-CDMA multipath fading channels," *Special Issue on Signal Processing for Wireless Communications* **16**, pp. 1765 – 1773, Dec 1998.

[11] J. S. Goldstein, I. S. Reed, and L. L. Sharf, "A multistage representation of the Wiener filter-based on orthogonal projections," *IEEE Trans.Inform. Theory* **44**, pp. 2943 – 2959, Nov 1998.

[12] D. A. Pados and G. N. Karystinos, "An iterative algorithm for the computation of the MVDR filter," *IEEE Trans. Signal Processing* **49**, pp. 290–300, Feb 2001.

[13] B. D. V. Veen, "Adaptive convergence of linearly constrained beamformers based on the sample covariance matrix," in *IEEE Transactions on Signal Processing*, **33**, pp. 1470–1473, June 1991.

[14] H. Qian and S. N. Batalama, "Data-record-based criteria for the selection of an auxiliary-vector estimator of the MMSE/MVDR filter," *IEEE Trans. Commun* **51**, pp. 1700–1708, Oct 2003.